AD-A130 719   ADVANCED EXPERIMENTAL TECHNIQUES IN CRACK TIP ANALYSIS   1/1
(U) WASHINTTON UNIV SEATTLE DEPT OF MECHANICAL
ENGINEERING A S KOBAYASHI JUN 83 UWA/DME/TR-83/48

UNCLASSIFIED   N00014-76-C-0060   F/G 20/11   NL

END
FILMED
DTIC

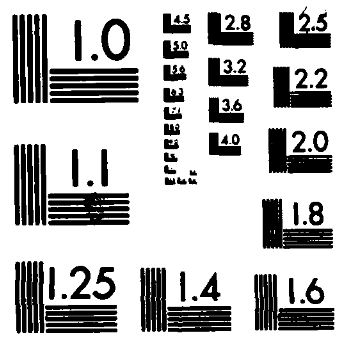

MICROCOPY RESOLUTION TEST CHART
NATIONAL BUREAU OF STANDARDS-1963-A

ADA130719

(12)

Office of Naval Research

Contract N00014-76-0060 NR 064-478

Technical Report No. UWA/DME/TR-83/48

ADVANCED EXPERIMENTAL TECHNIQUES IN CRACK TIP ANALYSIS

by

A. S. Kobayashi

June 1983

DTIC FILE COPY

The research reported in this technical report was made possible through support extended to the Department of Mechanical Engineering, University of Washington, by the Office of Naval Research under Contract N00014-76-C-0060 NR 064-478. Reproduction in whole or in part is permitted for any purpose of the United States Government.

Department of Mechanical Engineering

College of Engineering

University of Washington

ADVANCED EXPERIMENTAL TECHNIQUES IN CRACK TIP MECHANICS

by

A. S. Kobayashi
University of Washington
Department of Mechanical Engineering
Seattle, Washington 98195

ABSTRACT

Advanced experimental techniques in crack tip mechanics are discussed under three categories of 2- and 3-D linear elastic, 2-D elasto-plastic and 2-D dynamic fracture mechanics. Specific techniques which were discussed are acousto-elasticity, frozen stress-moire technique, isodyne photoelasticity, moire technique, laser speckle method, hybrid experimental-numerical analysis and caustic method.

INTRODUCTION

The experimental techniques for crack tip mechanics of the 1970's were governed by the practical requirements for determining accurately 2- and 3-D stress intensity factors in linear elastic fracture mechanics (LEFM). The extensive applications of three-dimensional frozen-stress phototelasticity [1], interferometry [2] and moire method [3] yielded static stress intensity factors for complex boundary value problems, such as a corner flaw at a nozzle-cylinder junction and at a through hole [4] and a compact specimen [5]. Dynamic stress intensity factors determined by the extensive use of dynamic photoelasticity [6, 7] and dynamic caustics [8, 9] provided considerable insight to the controversial criteria for dynamic fracture and crack arrest. Dynamic photoelasticity and dynamic caustics were also used to establish dynamic crack curving and branching criteria [10, 11], which are also applicable to static and quasi-static crack problems, and to repudiate the proposed fracture mechanics interpretation of the V-notched Charpy data [12]. These experimental techniques, which are constantly being improved to determine well-defined physical quantities, i.e., the stress intensity factors, have contributed to the credibility which linear elastic fracture mechanics commands, in postmortem failure analysis and life-time prediction of structural components.

The inevitable extensions of linear elastic fracture mechanics to fracture of composites, fatigue crack extension and stable crack growth as well as ductile fracture have imposed a new role onto the above experimental techniques. The experimental results are now also used to identify the physical laws and associated physical parameters governing these fracture phenomena. The search for these unknown physical parameters requires increased experimental accuracy as well as advanced data processing technique in the presence of geometric and material nonlinearities encountered in nonlinear fracture mechanics.

The purpose of this paper is to review the advances made in the established experimental techniques as well as to report on new experimental techniques for analyzing the traditional as well as new problems in crack tip mechanics. The techniques are discussed under three categories of 2- and 3-D linear elastic, 2-D elasto-plastic and 2-D dynamic fracture mechanics.

2-D Linear Elastic Fracture Mechanics

Acousto-elasticity

Acousto-elasticity, which was hailed as an analog to photoelasticity for opaque materials in 1959 [13], failed to achieve wide acceptance due to the unresolved transducer coupling effect and high sonic attenuation [14]. The resurgence of acousto-elasticity in the 1980's is due in parts to improvements in the instrumentation techniques but is mainly attributed to the ability for processing large amounts of ultrasonic data by a computer-controlled scanning system [15]. Since longitudinal ultrasonic waves provide information only on plane-stress isopachics (sum of principal stresses), the use of shear waves measurements, which are referred to as acoustic birefringence, is more widely used today. Influence of the inherent acoustic anisotropy (texture) in the material can be modeled by orthotropic elasticity theory which involves three acousto-elastic constants [16, 17]. The acoustic birefringence equation becomes

$$B = \{[B_0 + M_1\ (\sigma_1 + \sigma_2) + M_2(\sigma_1 - \sigma_2)\cos 2\theta]^2 + [M_3(\sigma_1 - \sigma_2)\sin\ 2\theta]^2\}^{1/2} \qquad (1)$$

where B_0 is the initial birefringence of the unstressed state. M_1, M_2 and M_3 are the three acousto-elastic constants.

The angle between the initial and stressed acousto-elastic axes, which in general do not coincide with the principal stress axes, is

$$\tan 2\phi = \frac{M_3(\sigma_1 - \sigma_2)\sin 2\theta}{B_0 + M_1(\sigma_1 + \sigma_2) + M(\sigma_1 - \sigma_2)\cos 2\theta} \qquad (2)$$

The shear stress in the xy plane is then given by

$$\sigma_{xy} = \frac{B \sin 2\phi}{2M_3} \qquad (3)$$

Clark, Mignogna and Sanford [18] used the above relations to measure the stress intensity factor in a 2024-T351 aluminum compact specimen shown in Figure 1. A pulse-echo-overlap system, as shown in Figure 2, was used to determine point-by-point, the orientation of the acoustic axes and the acoustic birefringence in the 51 x 51 mm square region shown in Figure 1. A 10 MHz ac-cut quartz shear-wave transducer of 1.8-mm diameter was used in a manual scanning process. The estimated accuracy were approximately 5% and $\pm$ 2 degrees in birefringence and ϕ measurements, respectively.

The acousto-elastic birefringence generated from 66 data points in the square region was reconstructed and Sanford's procedure [19] was used to compute five coefficients in the LEFM crack tip stress field by averaging the results of 100 computations using 20 randomly selected data points each time. Good agreement between the corresponding coefficients, which were obtained from a similar photoelasticity experiment, were noted. The stress intensity factor was computed from the coefficient of the first term, or the $1/\sqrt{r}$ term, in the above polynomial crack tip stress field.

The acousto-elastic technique is one of the few static, stress analysis techniques available for opaque materials. As in 2-D photoelasticity, the thickness-averaged acoustic birefringence is not subject to the plane stress constraint of the caustic method. Obvious improvement in the technique can be made by incorporating an automated scanning procedure with real-time data processing which has been used by others [15]. Yet to be explored is the physical significance of acoustic birefringence associated with the crack tip plastic region associated with ductile fracture.

3-D Linear Elastic Fracture Mechanics

Frozen Stress-Moire Technique

The hybrid technique, which utilizes both frozen stress, 3-D photoelasticity and moire interferometry, provides the complete information for characterizing the crack tip state [20]. The procedure is redundant in that the in-plane displacement field, which is determined by the high resolution moire technique [21], also defines the strain and stress fields. The isochromatics, however, can be used to verify the accuracy of the stresses which are obtained by numerically differentiating the displacements. Such optimum use of the redundant experimental data is yet to be explored.

The procedure consists of applying an aluminum reflective grating to the slices cut from the frozen-stress 3-D photoelastic model and returning the slice to its unloaded stage by annealing through its critical temperature. The in-plane displacements are obtained by moire interferometry of the deformed grating superimposed onto an undeformed virtual grating with a grating density of 2400 lines per mm. Figure 3 shows experimental setup for viewing the Moire fringes. The in-plane displacements of u_n and u_z are related to the stress intensity factor by:

For plane strain,

$$u_n = \frac{K_{AP}}{G}\sqrt{\frac{r}{2\pi}}\cos\frac{\theta}{2}\left[1 - 2\nu + \sin^2\frac{\theta}{2}\right]$$

$$u_z = \frac{K_{AP}}{G}\sqrt{\frac{r}{2\pi}}\sin\frac{\theta}{2}\left[2 - 2\nu\cos^2\frac{\theta}{2}\right] \tag{4}$$

For plane stress,

$$u_n = \frac{K_{AP}}{G}\sqrt{\frac{r}{2\pi}}\ \sin\frac{\theta}{2}\left[\frac{1-\nu}{1+\nu} + \sin^2\frac{\theta}{2}\right]$$
$$u_z = \frac{K_{AP}}{G}\sqrt{\frac{r}{2\pi}}\ \sin\frac{\theta}{2}\left[\frac{2}{1+\nu} - \cos^2\frac{\theta}{2}\right] \qquad (5)$$

where G is shear modulus of elasticity,
ν is Poisson's ratio

The photoelastic-moire technique was used to determine the variation in stress intensity factor along a straight crack front in a four-point bend specimen of 279.4 x 25.7 x 13.3 mm size after ASTM E399. Figure 4 shows the stress intensity factors at the center slice of this cracked beam determined by both photoelasticity and moire interferometry for a crack depth to beam ratio of 0.5. The reference K_{th} in Figure 4 was determined by 2-D plane strain analysis [22]. Figure 5 shows the variation of stress intensity factor through the thickness of the beam. A state of plane stress and the presence of a $1/\sqrt{r}$ singularity were assumed in the data reduction process.

While the uncertainties in the relaxation mechanism as well as the resultant state of stress associated with the annealing process require further studies, the frozen stress-moire techniques provides a mean for complete and detailed stress analysis of the crack tip state in 3-D linear elastic fracture mechanics.

Isodyne Photoelasticity

Isodyne represents curves of constant intensity of the normal forces acting on the characteristic curves in a plane stress field and are thus related to the first derivatives of the Airy stress function. Two isodyne fields related to two orthogonal characteristic curves completely define the elastic state of plane stress [23]. When modeled optically with the integrated polariscope, shown in Figure 6 [24], the photoelastic isodynes resemble the isochromatics generated by scattered light photoelasticity. Similar to scattered light photoelasticity, optical inhomogeneity generated by the high stress gradient in the vicinity of the crack tip may distort the photoelastic isodyne. The requirement for a plane stress state, which is not a prerequisite in scattered light photoelasticity, can be modulated by the "semi-plane stress state" used by Pindera et al. [25] who then determined the stress intensity factor at the midsection, i.e. plane of symmetry, of a four-point bend specimen shown in Figure 7. Also shown in Figure 7 is the variation in the stress intensity factor computed for various crack tip distance where a pronounced effect of the near-tip nonlinearity and crack tip bluntness are noted.

Asssuming that the influence of optical inhomogeneity in the scattered light path can be quantified, the photoelastic isodyne technique share the same advantage of 3-D scattered photoelasticity which can be used to analyze the crack tip state of stress under live load. The stress intensity factor can be computed more accurately if K is expressed directly in terms of the isodyne value thus eliminating the extra numerical differentiation process in obtaining the stresses.

2-D Elasto-Plastic Fracture Mechanics

The experimental techniques listed in this section obviously can be used for elastic analysis but unlike the above, are not limited to elastic analysis.

Moire Technique

The use of moire technique in elasto-plastic fracture mechanics is not new [3, 26]. Despite its obvious application to high temperature, nonlinear problems in fracture mechanics, literature is relatively sparse in the fracture mechanics interpretation of the crack tip displacement field determined by the moire method. Exception to the above is the analysis of externally notched rings sliced from a Type 304 stainless tube, 7.1-mm O.D. and 0.38 mm thick, with electro-etched cross-line gratings of 40 lines per mm and subjected to a simulated internal pressure at 1100 F [27]. Figure 8 shows the experimental setup for recording the distorted grating which was analyzed by master gratings of 4 and 8 lines/mm. From the resultant u and v moire fringe patterns, COD for slow-crack growth initiation was found to be

$$COD = 0.976 \cdot a \cdot \sigma^{5.78} \tag{6}$$

where the crack length a and the applied hoop stress ϕ are represented in terms of mm and KN, respectively.

Figure 9 shows that the initiation COD in this experiment remained relatively constant despite the changes in the crack tip bluntness. Sciammarella then estimated the J-integral for the initiation of slow crack growth by the following approximate formula after Rice et al. [28].

$$J_{in} = \frac{1}{bt} [2 \int_0^{bcr} Pd\delta_{cr} - Pr\delta_{cr}] \tag{7}$$

where b is the ligament length, t is the specimen thickness, δ_{cr} is the displacement due to the presence of the crack between two reference sections for the load at the moment of crack initiation and

$$P = \sigma A \tag{8}$$

where σ is the hoop stress and A the specimen cross-sectional area. The values of δ_{cr} were obtained as

$$\delta_{cr} = \delta_{total} - \delta_{nocr} \tag{9}$$

where δ_{total} is the displacement between two reference cross sections and δ_{nocr} is the displacement given by

$$\delta_{nocr} = \Delta\epsilon_h \tag{10}$$

Moire method, which was limited in its applications to fracture problems involving large scale yielding due its low sensitivity, can be used in the high sensitivity region of linear elastic fracture mechanics by the recent developments in high density line gratings upto 4000 lines per mm with grating sizes upto 100 x 63 mm [29]. The use of virtual grating, which was described previously, eliminates the need for physical contact of the reference grating. Its use at elevated temperature testing, such as that described above, or under an explosive loading condition may be in doubt since the long optical paths, which is required in the experimental setup, may be distorted by the

TABLE I

J_{in} For Ring Specimen at 1100°F

Ring No.	$P \cdot \delta$, KN·cm	J_{in} MJ/m^2
1	0.0682	0.03980
2	0.0565	0.05554
3	0.0455	0.04755
4	0.0661	0.04520
5	0.0517	0.04762
6	0.0298	0.02206
7	0.0684	0.04681
8	0.0421	0.03484
9	0.0709	0.04742

Table 1 shows the excess variations in the J estimated by this procedure thus leading this author to conclude that COD is a better criterion for predicting the initiation of slow crack growth.

moving air current or shock waves.

The moire fringes can be generated by holographic interferometry. Referred to as "intrinsic holographic moire", these fringes can be recorded by using the basic setup shown in Figure 10 [30]. The reference state is obtained by a single exposure of the unloaded specimen. Rigid body motions of the loaded specimen are compensated by displacing the reference state and observing the fringe contrast in the TV monitor. The u and v fringe patterns are recorded on tape or alternatively photographed directly.

Laser Speckle Method

Despite its many implied applications in fracture mechanics [31, 32], literature is void of useful data which has been generated by the speckle method. With its high sensitivity, i.e. u and v displacement measurements of the order of 0.005 mm, the laser speckle method should find wide ranging applications in experimental fracture mechanics. By using the digital imaging technique [33, 34] to cross correlate the two speckle images generated by the unloaded and loaded specimens, the method provides an efficient procedure for processing the immense amount of data and for easy access to graphic peripherals.

Hybrid Experimental-Numerical Analysis

One of the major obstacle, which hinders the progress of experimental ductile fracure research, is the undefined crack-tip states of stress and strain in the presence of large scale yielding. Since the $1/\sqrt{r}$ singular state in linear elastic fracture mechanics is a physical impossibility which successfully models brittle fracture, similar phenomenological model could be developed for a crack under large scale yielding. A popular and possibly over-exploited such model is the Dugdale strip yield zone which conveniently reduces the elastic-plastic crack-tip state to an elastic one. The Dugdale strip yield model used in a recent analysis [37] is a modification of the classical Dugdale model where higher order terms were added to increase the number of disposable parameters. Experimental data is then used to fit the disposal parameters associated with the Dugdale model, which is modified to fit the complex state associated with large scale yielding, just as the stress intensity factor is determined from photoelasticity and moire fringe data. The adequacy of such model can be verified by the matching other crack-tip data which is not used in the fitting process but which is generated numerically by the Dugdale model and independently by the experiment. The extensive numerical experimentation neccessary for this verification study in essence replaces the finite element or boundary element method used in the traditional hybrid experimental-numerical stress analysis technique [36]. The verified modified Dugdale model through the generation mode of hybrid experimental-numerical analysis can then be used to generate numerically various fracture parameters for evaluation.

The utility of the hybrid experimental-numerical analysis is demonstrated by a recent investigation on stable-crack growth under mixed-mode loading [37]. Isochromatics in a 1.6-mm thick polycarbonate tensile specimens with central slanted crack were recorded during a continuing stable crack growth period. The resultant Z-shaped crack was modeled by a straight Dugdale crack, which was modified to account for the residual stresses left behind in the wake of the rapidly extending crack, as shown in Figure 11. The modification consisted of two unknown tangential forces acting at the physical crack tip. Lengths of the Dugdale strip yield zones ahead of the crack tip were measured from the photoelastic records [37]. These lengths coincided with the length of the theoretical values of the horizontal crack thus justifying the use of the model of Figure 11 to represent the Z-shaped cracks. The crack-tip stress field which is represented by a polynomial stress function of the crack-tip coordinates together with the two unknown tangential forces were fitted to the recorded elastic isochromatics surrounding the plastic region using an overdeterministic fitting routine [38]. Figure 12 shows the near- and far-field isochromstics which were regenerated by using the modified Dugdale model and those obtained by photoelasticity. Figure 13 shows the crack tip opening angle (CTOA), which was computed by using the modified Dugdale model, for the two intial crack geometries to be almost constant during the stable crack growth process.

While the hybrid experimental-numerical technique may not provide the micromechanics insight to crack-tip mechanics, it can be used to effectively extract fracture parameters which other wise cannot be measured directly.

Caustic Method

The method of caustics is becoming a popular technique for measuring the static and dynamic stress intensity factors for plane-stress problems in linear elastic fracture mechanics. Caustic can also be generated by any deformed specimen surface including the obvious dimpling surrounding a ductile crack. Rosakis and Freund [39] used an asymptotic elastic-plastic analysis to relate this dimpling to a plastic intensity factor. By postulating an HRR singularity, J-deformation theory of plasticity and the separation of theta and r, the plastic strain in the thickness direction is obtained as

$$\varepsilon_{33}^{p} = -\left(\varepsilon_{rr}^{p} + \varepsilon_{\theta\theta}^{p}\right) \tag{11}$$

where the in-plane plastic strain components are given in terms of the stress components as

$$e_{rr}^{p} = \frac{\alpha\sigma_0}{E}\left[\frac{JE}{\alpha\sigma_0^2 I_n r}\right]^{\frac{n}{n+1}}\left(\frac{\sigma_e}{\sigma_0}\right)^{n-1}\left(\Sigma_{rr} - \frac{1}{2}\Sigma_{\theta\theta}\right) \tag{12}$$

The resultant caustic generated by the thickness direction strain of equation (12) is shown in Figure 14. J-integral value can then be determined by

$$e_{\theta\theta}^{p} = \frac{\alpha\sigma_0}{E}\left[\frac{JE}{\alpha\sigma_0^2 I_n r}\right]^{\frac{n}{n+1}}\left(\frac{\sigma_e}{\sigma_0}\right)^{n-1}\left(\Sigma_{\theta\theta} - \frac{1}{2}\Sigma_{rr}\right) \tag{13}$$

where z_0, d and σ_0 are the screen distance, specimen thickness and tensile yield stress, respectively.

While further verification study is necessary, the caustic method promises to provide an experimental procedure with which, the J-value can be determnined directly using crack tip measurements in contrast to the ASTM designated far-field procedure which is based on many simplifying assumptions.

2-D Dynamic Fracture Mechanics

As mentioned in the Introduction, literature is abundant with experimental results on linear elastic dynamic fracture using dyanmic photoelasticity and dynamic caustics. Experimental as well as data processing procedures for these two techniques are continually being improved and their domain of application is being extented. One such extension is the use of the hybrid experimental-model analysis for modeling the Dugdale strip yield zone ahead of a rapidly tearing crack [37]. Likewise, the caustic method with its asymptotic elastic-plastic solution could be extended with relative ease to analyze problems involving rapid tearing.

CLOSING COMMENTS

While no claim is made for completeness, most of the significant new experimental techniques for crack tip mechanics hopefully have been mentioned in this paper. The potential of applying some of the 2-D techniques, which were listed under specific fields in crack tip mechanics, to other fields obviously must be explored.

ACKNOWLEDGEMENT

The work reported here was obtained under ONR Contract N00014-76-C-0060 NR 064-478. The authors wish to acknowledge the support and encouragement of Dr. Y. Rajapakse, ONR during the course of this investigation.

REFERENCES

1. SMITH, C. W., "Use of Three-dimensional Photoelasticity and Progress in Related Areas", Experimental Techniques in Fracture Mechanics, 2, ed by A. S. Kobayashi, Society for Experimental Stress Analysis, 1975, pp 3 - 58.

2. PACKMAN, P. F., "The Role of Interferometry in Fracture Studies", ibid loc cit, pp 59 - 87.

3. LIU, H. W. and KE, J.S., "Moire Method", ibid loc cit, pp 111 - 165.

4. SMITH, C. W., POST, D. and NICOLETTO, G., "Prediction of Sub-critical Crack Growth from Model Experiments", Developments in Theoretical and Applied Mechanics, ed by T. J. Chung and G. R. Karr, The University of Alabama in Huntsville, 1982, pp 167 - 179.

5. FOURNEY, M. E., "Experimental Determination of the effect of Crack Front Curvature in an ASTM Compact Tension Speciment", Proc. of the Fourth Brazilian Congress of Mechanical Engineering, 1977, pp 13 - 26.

6. DALLY, J. W., "Dynamic Photoelastic Studies of Fracture", Experimental Mechanics, Vol. 19, 1979, pp 349 - 361.

7. BRADLEY, W. B. and KOBAYASHI, A. S., "Fracture Dynamics - A Photoelastic Investigation", J. of Engineering Fracture Mechanics, Vol. 3, 1971, pp 317 - 332.

8. KALTHOFF, J. F., BEINERT, J. and WINKLER, S., "Measurements of Dynamic Stress Intensity Factors for fast Running and Arresting Cracks in double Cantilever-beam Specimens", Fast Fracture and Crack Arrest, ed by G. T. Hahn and M. F. Kanninen, ASTM STP 627, 1977, pp 161 - 176.

9. THEOCARIS, P. S., "Optical method of caustics in the study of dynamic problems of running cracks", Optical Engineering, Vol. 21, July/August 1982, pp 581 - 601.

10. RAMULU, M. and KOBAYASHI, A. S., "Dynamic Crack Curving - A Photoelastic Evaluation", Experimental Mechanics, Vol. 22,3, March 1983, pp 1 - 9.

11. RAMULU, M., KOBAYASHI, A. S. and KANG, B. S.-J., "Dynamic Crack Branching - A Photelastic Evaluation", to be published in ASTM STP.

12. KALTHOFF, J. F., WINKLER, S., BOHME, W. and KLEMM, W., "Measurements of Dynamic Stress Intensity Factors in Impacted Bend Specimens", C.S.N.I. Specialist Meeting on Instrumented Precracked Charpy Testing, ed by R. A. Wullaert, Electric Power Research Institute, EPRI NP-2102-LD, Nov. 1981, pp 2-3 - 2-19.

13. BENSON, R. W. and RAELSON, V. J., "Acoustoelasticity", Product Engineering, Vol. 30, 1959, pp 56 - 59.

14. BLINKA, J. and SACHSE, "Application of Ultrasonic-pulse-spectroscopy Measurements to Experimental Stress Analysis", Experimental Mechanics, Vol. 16, Dec. 1976, pp 448 - 453.

15. KINO, G. S., HUNTER, J. B., JOHNSON, G. C., SELFRIDGE, A. R., BARNETT, D. M., HERMAN, G. AND STEELE, C. R., "Acoustoelastic Imaging of Stress Fields", J. of Applied Physics, Vol. 50, (4) April, 1979 pp. 530-535.

16. OKADA, K., "Stress-Acoustic Relation for Stress Measurements by Ultrasonic Technique", J. of Acoustical Soc. of Japan (E), Vol. 1, No. 3, 1980, pp 193 - 200.

17. OKADA, K., "Acoustoelastic Determination of Stress in Slightly Orthotropic Materials", Experimental Mechanics, Vol. 21, 1981, pp 461 - 466.

18. CLARK, A. V., MIGNOGNA, R. B. and SANFORD, R. J., "Acousto-elastic Measurement of Stress and Stress Intensity Factors Around Crack Tips", Ultrasonics, March 1983, pp 57 - 64.

19. SANFORD, R. J. and CHONA, R., "An Analysis of Photoelastic Fracture Patterns with Sampled Least-squares Methods, Proc. of the 1981 SESA Spring Meeting, SESA, June 1981, pp 273 - 276.

20. SMITH, C. W., POST, D. and NICOLETTO, G., "Experimental Stress Intensity Distributions in Three Dimensional Cracked Body Problems", Proc. of Joint Conference on Experimental Mechanics, SESA, May 1982, pp 196 - 200.

21. NICOLETTO, G., POST, D. and SMITH, C. W., "Moire Interferometry for High Sensitivity Measurements in Fracture Mechanics", ibid loc cit, pp 266 - 270.

22. "Standard E399 on Fracture Toughness Testing", Annual Book of ASTM Standards, Part 10 Metals, 1981, pp 605 - 607.

23. PINDERA, J. T., "New development in photoelastic studies: isodyne and gradient photoelasticity", Optical Engineering, Vol. 21, July/Aug 1982, pp 672 - 678.

24. MAZURKIEWICS, S. B. and PINDERA, J. T, "Integrated Plane Photoelastic Method - Application of Photoelastic Isodynes", Experimental Mechanics, Vol. 19, July 1979, pp 225 - 234.

25. PINDERA, J. T., KRASNOWSKI, B. R. and PINDERA, M.-J., "An Analysis of Semi-plane Stress States in Fracture Mechanics and Composite Structures Using Isodyne Photoelasticity", Proc. of the 1982 Joint Conf. on Experimental Mechanics, SESA, May 1982, pp 417 -421.

26. HU, W. L. and LIU, H. W., "Crack Tip Strain - A Comparison of Finite Element Calculations and Moire Measurements", Cracks and Fracture, ed by J. L. Swedlow and M. L. Williams, ASTM STP 601, 1976, pp 622 - 534.

27. SCIAMMARELLA, C. A. and RAO, M. P. K., "Failure Analysis of Stainless Steel at Elevated Temperatures", Experimental Mechanics, Vol. 19, 1979, pp 389 -398.

28. RICE, J. R., PARIS, P. C. and MERKLE, J. G., "Some Further Results on J-Integral Analysis and Estimates", Progress in Flaw Growth and Fracture Toughness Testing, ASTM STp 536, 1973, pp 231 - 245.

29. POST, D., "Developments in moire interferometry", Optical Engineering, Vol. 21, May/June 1982, pp 458 - 467.

30. SCIAMMARELLA, C. A., "Holographic moire, an optical tool for the determination of displacements, strains, contours and slopes of surfaces", ibid loc cit, pp 447 -457.

31. CHIANG, F. P., ADACHI, J., ANASTASI, R. and BEATTY, J., "Subjective laser speckle method and its application to solid mechanics problems", ibid loc cit, pp 379 - 390.

32. BOONE, P. M., "Use of close range objective speckles for displacement

measurement", ibid loc cit, pp 407 - 410.

33. PETERS, W. H. and RANSON, W. F., "Digital imaging techniques in experimental stress analysis", ibid loc cit, pp 427 -431.

34. MCNEIL, S. R., PETERS, W. H., RANSON, W.F. and SUTTON, M. A., "Digital-Image Processing in Fracture Mechanics", a paper presented at the 1983 SESA Spring Meeting, Cleveland, May 1983.

35. KOBAYASHI, A. S. and LEE, O. S., "Elastic Field Surrounding a Rapidly Tearing Crack", to be published in Elastic-Plastic Fracture Mechanics, ASTM STP, 1983.

36. KOBAYASHI, A. S., "Hybrid Experimental-Numerical Stress Analysis", to be published in Experimental Mechanics.

37. SUN, Y. J., LEE, O. S. AND KOBAYASHI, A. S., "Crack Tip Plasticity Under Mixed-mode Loading", to be published in the Proc. of The ICF Symposium on Fracture Mechanics, Beijing, China, Nov. 1983.

38. BETSER, A. A., KOBAYASHI, A. S., LEE, O. S. and KANG, B. S.-J., "Crack Tip Dynamic Isochromatics in the Presence of Small Scale Yielding", Experimental Mechanics, Vol. 22, 1982, pp. 132-138.

39. ROSAKIS, A. J. and FREUND, L. B., "Optical Measurement of Plastic Strain Concentration at a Crack Tip in a Ductile Steel Plate", ASME J. of Applied Mechanics, Vol. 104, April 1982, pp. 115-120.

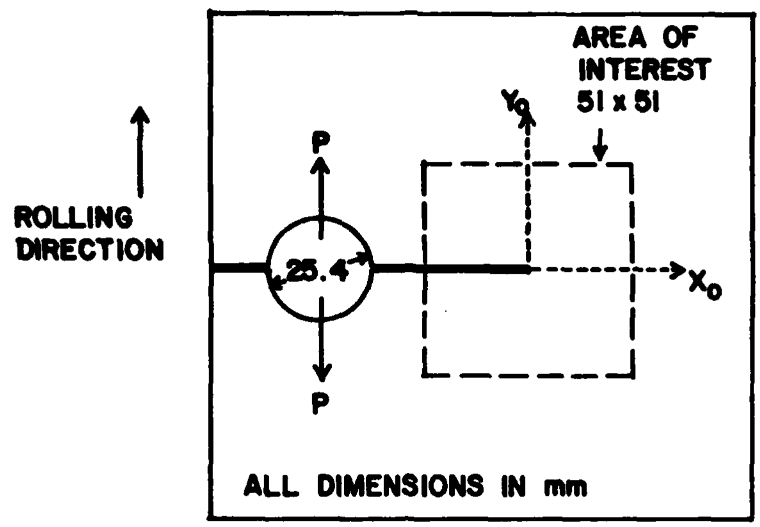

Fig. 1 Schematic diagram of the modified compact tensile specimen. The region where acoustic measurements were made is labelled 'area of interest'. Also shown are the initial acoustic axes, X_0 and Y_0.

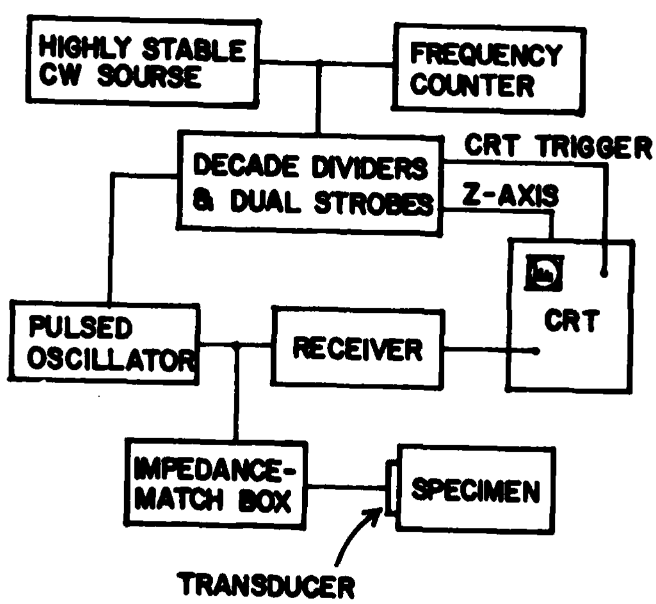

Fig. 2 Block diagram of pulse-echo-overlap system.

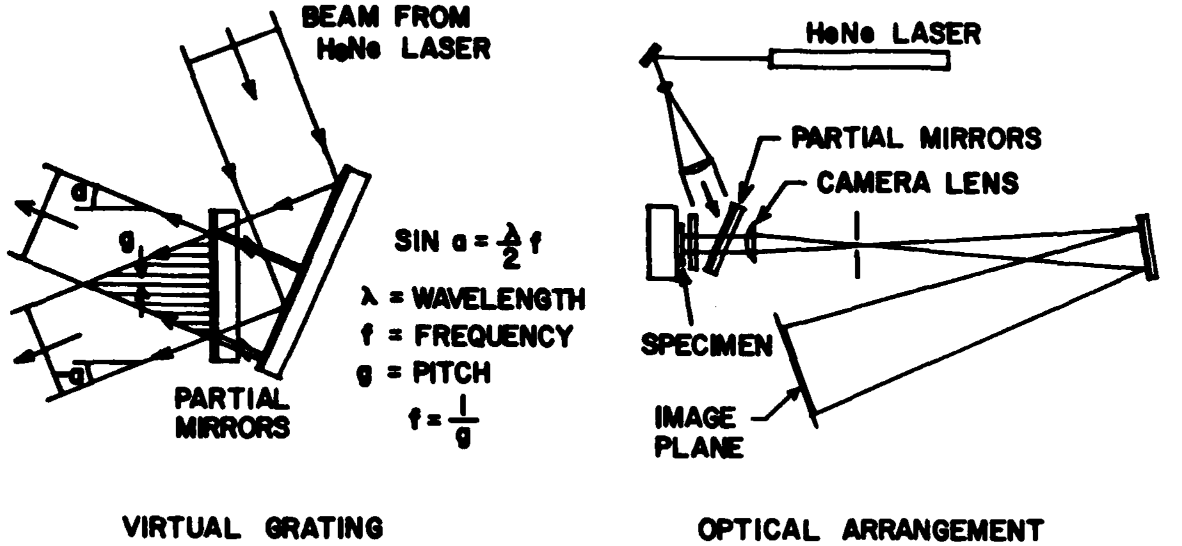

Fig. 3 Setup for Moire interferometry.

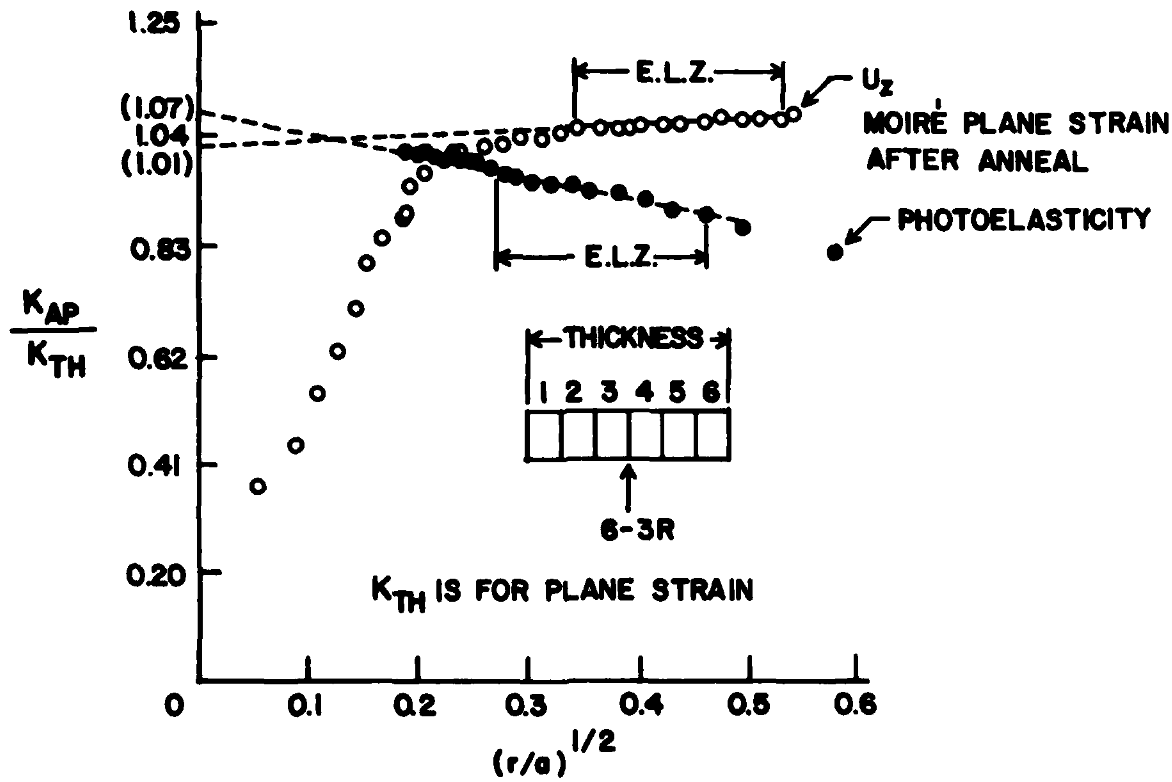

Fig. 4 Comparison of Photoelastic and Moire Results.

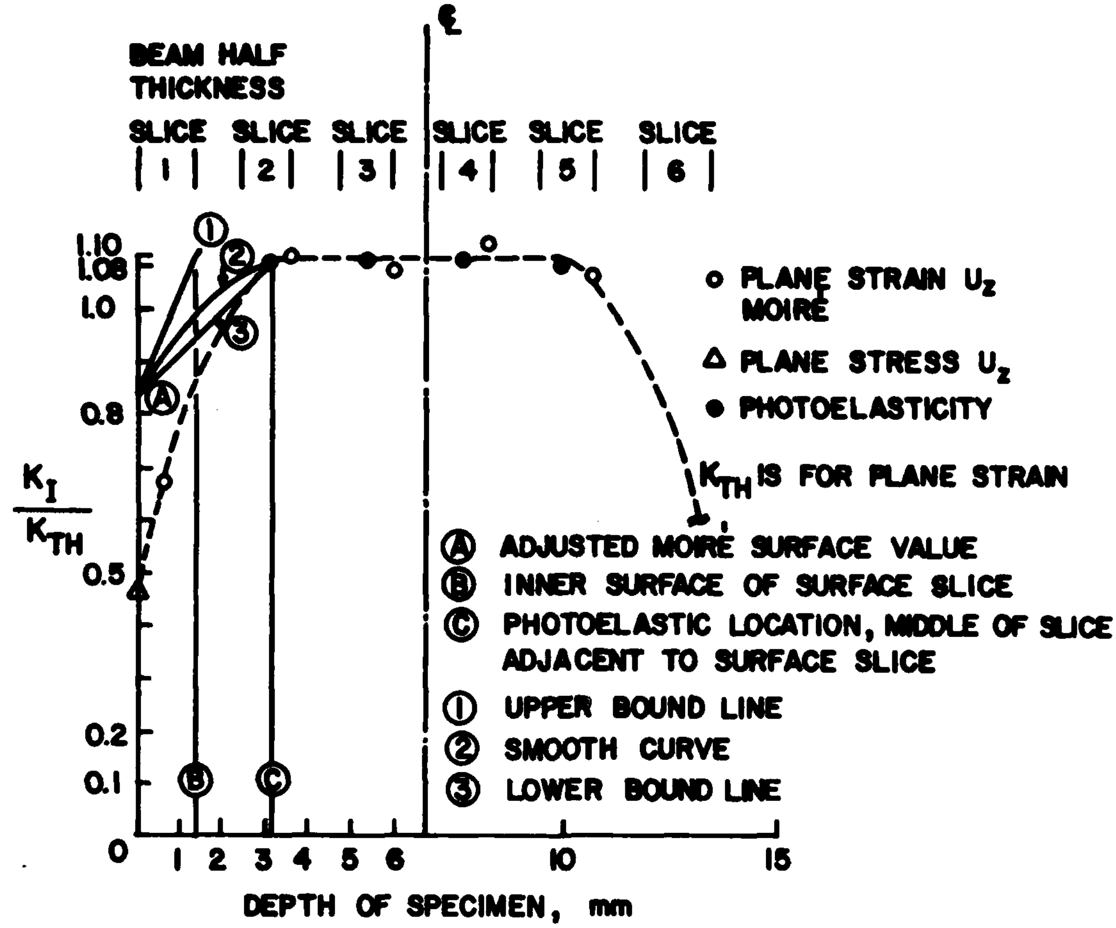

Fig. 5 SIF distribution across the thickness (a/W = 0.50)

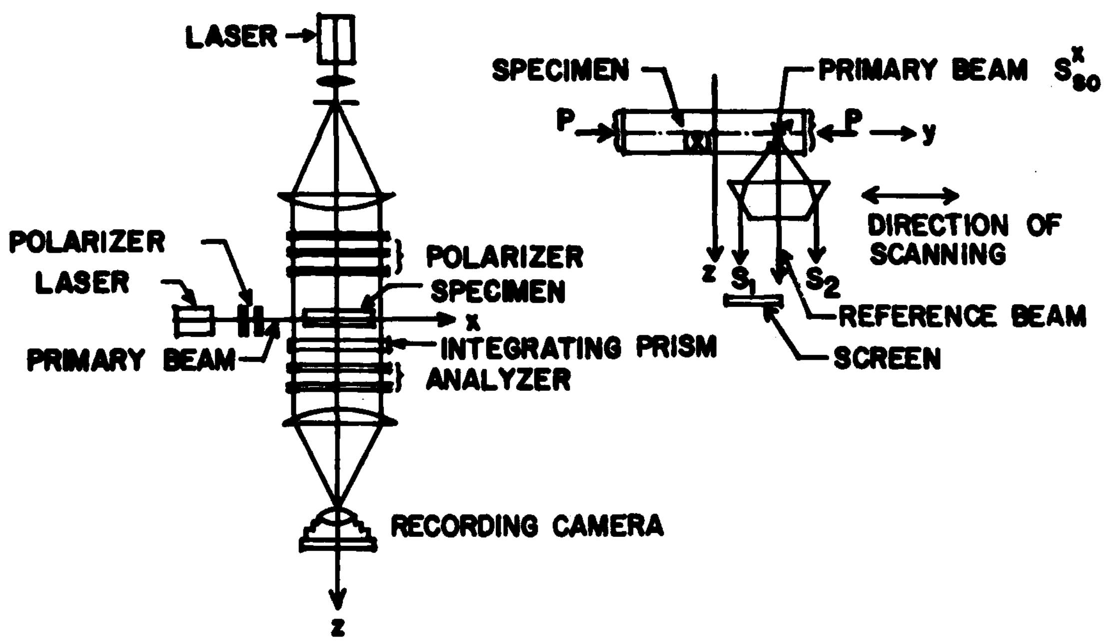

Fig. 6 Integrated Polariscope for isodyne photoelasticity

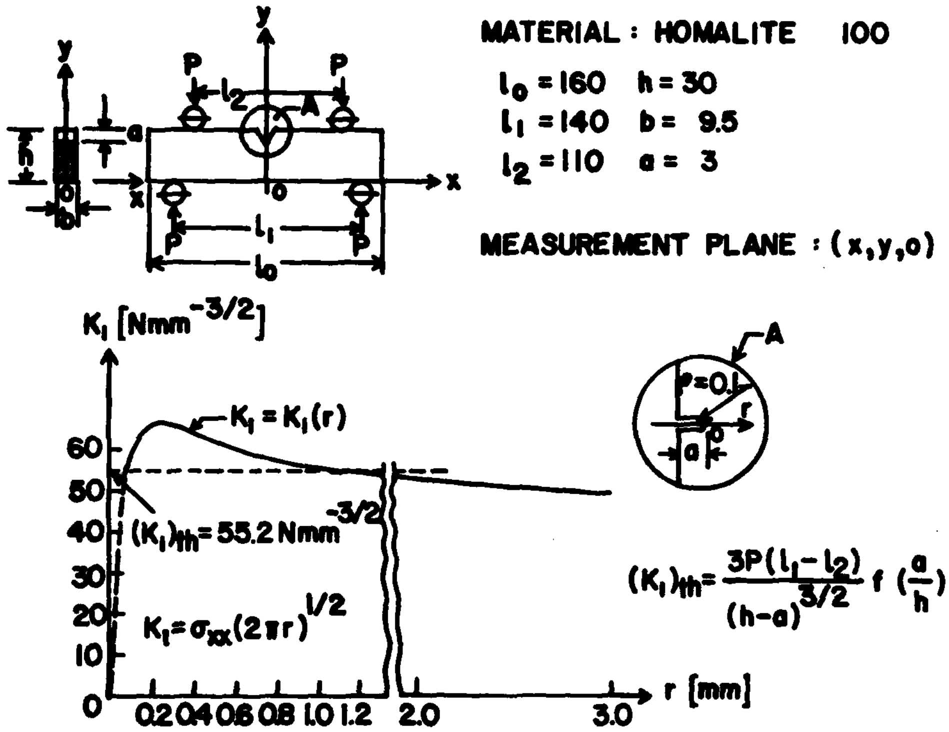

Fig. 7 Four point bend beam with sharp notch. $K_I(r)$ for central plane was determined by isodyne technique.

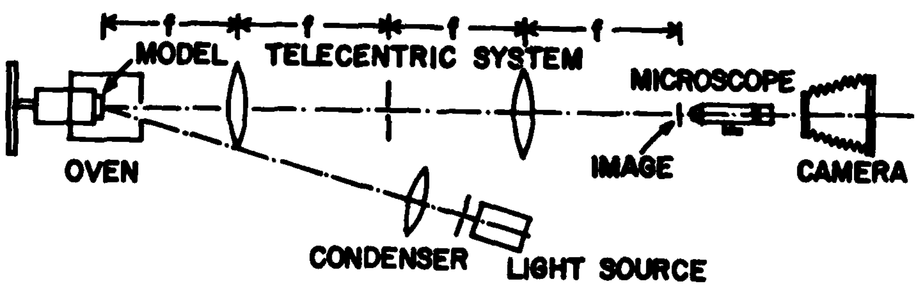

Fig. 8 Optical setup for high-temperature studies.

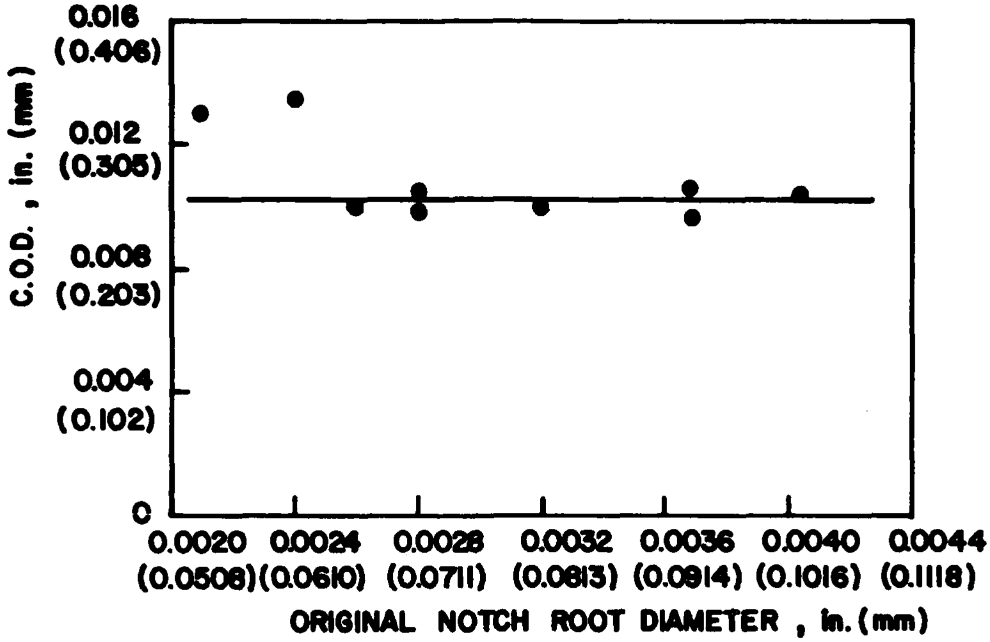

Figure 9 C.O.D. for the initiation of slow crack growth as a function of original notch-root diameter.

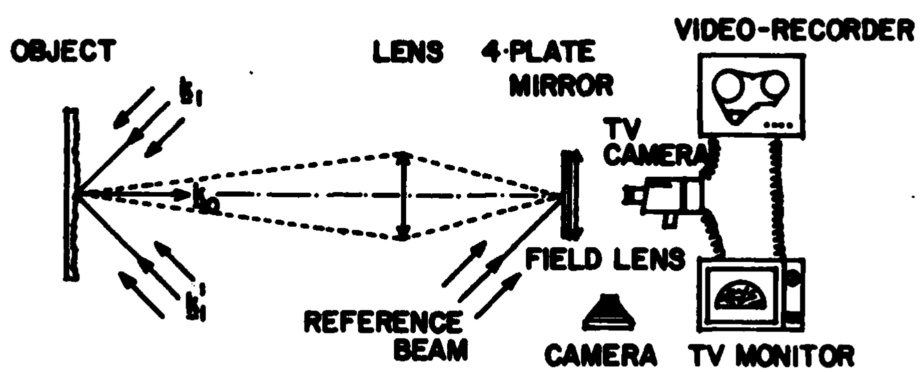

Fig. 10 Schematic representation of the recording system in image plane holography.

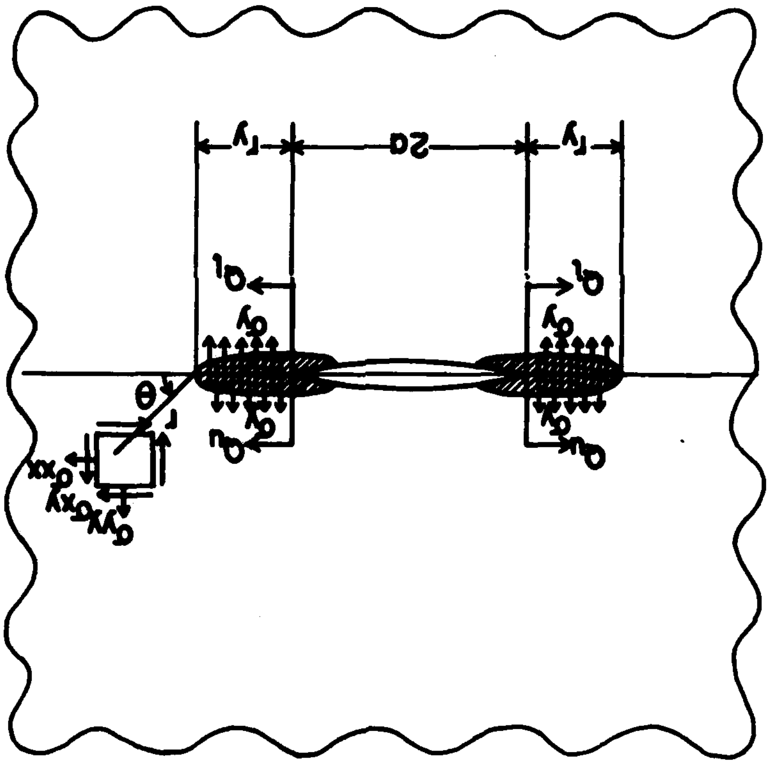

Fig. 11 Modified Dugdale strip yield model.

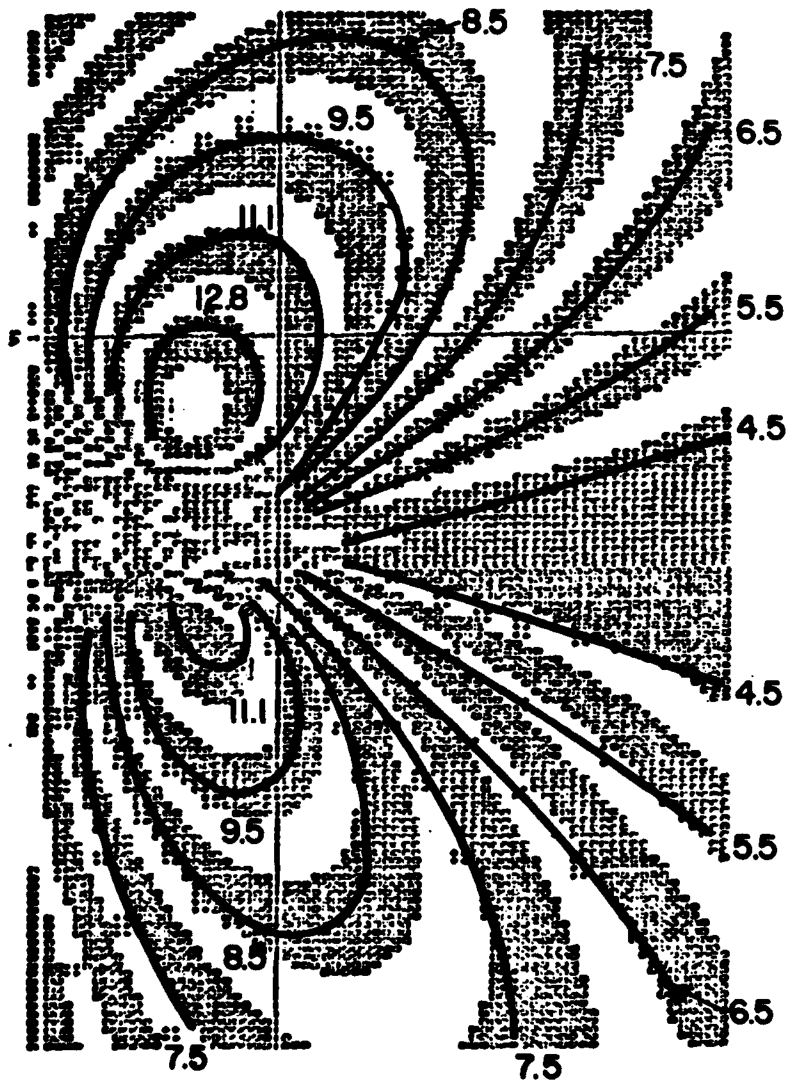

Fig. 12 Computer generated and actual (solid curves) Isochromatics 30° SCN specimen

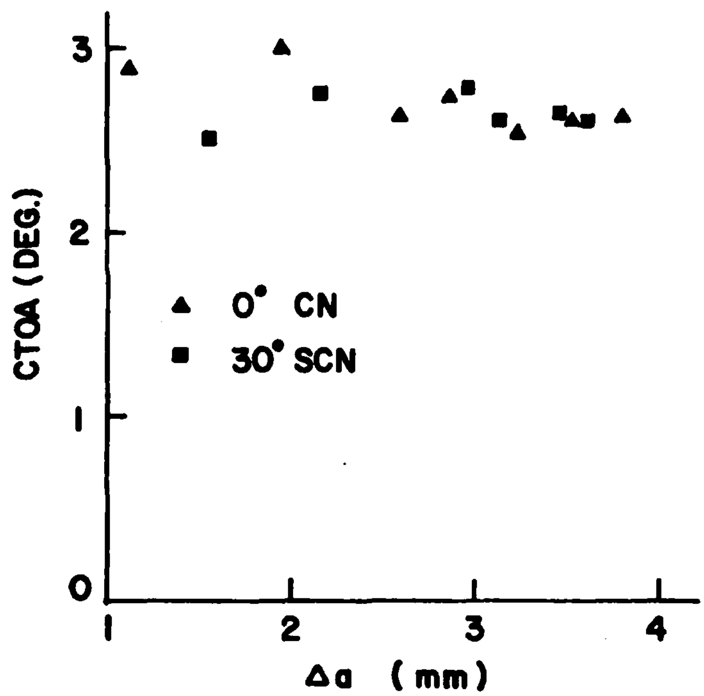

Fig. 13 CTOA during stable crack growth of 0° CN and 30° SCN.

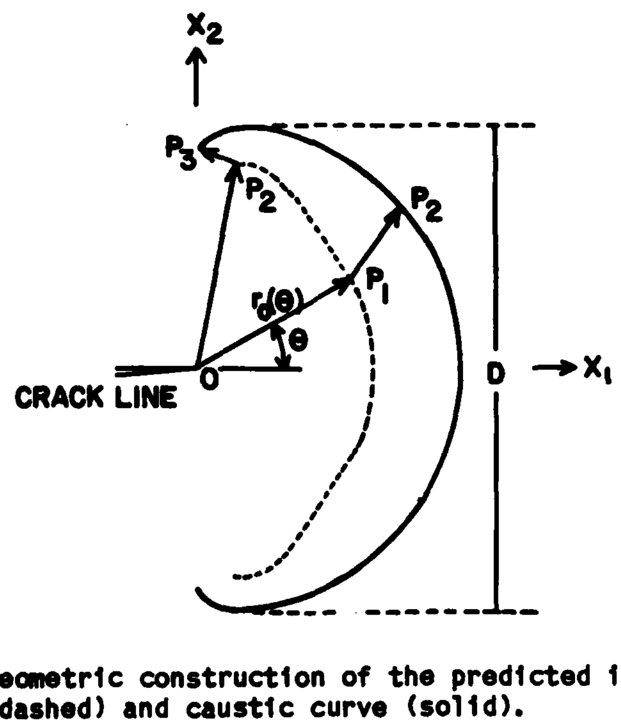

Fig. 14 Geometric construction of the predicted initial curve (dashed) and caustic curve (solid).

Part 1 - Government
Administrative and Liaison Activities

Office of Naval Research
Department of the Navy
Arlington, VA 22217
Attn: Code 474 (2)
471
200

Director
Office of Naval Research
Branch Office
666 Summer Street
Boston, MA 02210

Director
Office of Naval Research
Branch Office
536 South Clark Street
Chicago, IL 60605

Director
Office of Naval Research
Branch Office
1030 East Green Street
Pasadena, CA 91106

Naval Research Laboratory (6)
Code 2627
Washington, D.C. 20375

Defense Documentation Center (12)
Cameron Station
Alexandria, Virginia 22314

Navy

Undersea Explosion Research Division
Naval Ship Research and Development
Center
Norfolk Naval Shipyard
Portsmouth, VA 23709
Attn: Dr. E. Palmer, Code 177

Navy (Con't.)

Naval Research Laboratory
Washington, D.C. 20375
Attn: Code 8400
8410
8430
8440
6300
6390
6380

David W. Taylor Naval Ship Research
and Development Center
Annapolis, MD 21402
Attn: Code 2740
28
281

Naval Weapons Center
China Lake, CA 93555
Attn: Code 4062
4520

Commanding Officer
Naval Civil Engineering Laboratory
Code L31
Port Hueneme, CA 93041

Naval Surface Weapons Center
White Oak
Silver Spring, MD 20910
Attn: Code R-10
G-402
K-82

Technical Director
Naval Ocean Systems Center
San Diego, CA 92152

Navy Underwater Sound
Reference Division
Naval Research Laboratory
P.O. Box 8337
Orlando, FL 32806

Navy (Con't.)

Chief of Naval Operations
Department of the Navy
Washington, D.C. 20350
Attn: Code OP-098

Strategic Systems Project Office
Department of the Navy
Washington, D.C. 20376
Attn: NSP-200

Naval Air Systems Command
Department of the Navy
Washington, D.C. 20361
Attn: Code 5302 (Aerospace and Structures)
604 (Technical Library)
320B (Structures)

Naval Air Development Center
Warminster, PA 18974
Attn: Aerospace Mechanics
Code 606

U.S. Naval Academy
Engineering Department
Annapolis, MD 21402

Naval Facilities Engineering Command
200 Stovall Street
Alexandria, VA 22332
Attn.: Code 03 (Research & Development)
04B
045
14114 (Technical Library)

Naval Sea Systems Command
Department of the Navy
Washington, D.C. 20362
Attn: Code 05H
312
322
323
05R
32R

Navy (Con't.)

Commander and Director
David W. Taylor Naval Ship
Research and Development Center
Bethesda, MD 20084
Attn: Code 042
17
172
173
174
1800
1844
012.2
1900
1901
1945
1960
1962

Naval Underwater Systems Center
Newport, RI 02840
Attn: Dr. R. Trainor

Naval Surface Weapons Center
Dahlgren Laboratory
Dahlgren, VA 22448
Attn: Code G04
G20

Technical Director
Mare Island Naval Shipyard
Vallejo, CA 94592

U.S. Naval Postgraduate School
Library
Code 0384
Monterey, CA 93940

Webb Institute of Naval Architecture
Attn: Librarian
Crescent Beach Road, Glen Cove
Long Island, NY 11542

Army

Commanding Officer (2)
U.S. Army Research Office
P.O. Box 12211
Research Triangle Park, NC 27709
Attn: Mr. J. J. Murray, CRD-AA-IP

Army (Con't.)

Watervliet Arsenal
MAGGS Research Center
Watervliet, NY 12189
Attn: Director of Research

U.S. Army Materials and Mechanics
Research Center
Watertown, MA 02172
Attn: Dr. R. Shea, DRXMR-T

U.S. Army Missile Research and
Development Center
Redstone Scientific Information
Center
Chief, Document Section
Redstone Arsenal, AL 35809

Army Research and Development
Center
Fort Belvoir, VA 22060

NASA

National Aeronautics and Space
Administration
Structures Research Division
Langley Research Center
Langley Station
Hampton, VA 23365

National Aeronautics and Space
Administration
Associate Administrator for Advanced
Washington, D.C. 20546

Air Force

Wright-Patterson Air Force Base
Dayton, OH 45433
Attn: AFFDL (FB)
(FBR)
(FBE)
(FBS)
AFML (MBM)

Air Force (Con't.)

Chief Applied Mechanics Group
U.S. Air Force Institute of Technology
Wright-Patterson Air Force Base
Dayton, OH 45433

Chief, Civil Engineering Branch
WLRC, Research Division
Air Force Weapons Laboratory
Kirtland Air Force Base
Albuquerque, NM 87117

Air Force Office of Scientific Research
Bolling Air Force Base
Washington, D.C. 20332
Attn: Mechanics Division

Department of the Air Force
Air University Library
Maxwell Air Force Base
Montgomery, AL 36112

Other Government Activities

Commandant
Chief, Testing and Development Division
U.S. Coast Guard
1300 E Street, NW.
Washington, D.C. 20226

Technical Director
Marine Corps Development
and Education Command
Quantico, VA 22134

Director Defense Research
and Engineering
Technical Library
Room 3C128
The Pentagon
Washington, D.C. 20301

Other Government Activities (Con't.)

Dr. M. Gaus
National Science Foundation
Environmental Research Division
Washington, D.C. 20550

Library of Congress
Science and Technology Division
Washington, D.C. 20540

Director
Defense Nuclear Agency
Washington, D.C. 20305
Attn: SPSS

Mr. Jerome Persh
Staff Specialist for Materials
and Structures
OUSDR&E, The Pentagon
Room 3D1089
Washington, D.C. 20301

Chief, Airframe and Equipment Branch
FS-120
Office of Flight Standards
Federal Aviation Agency
Washington, D.C. 20553

National Academy of Sciences
National Research Council
Ship Hull Research Committee
2101 Constitution Avenue
Washington, D.C. 20418
Attn: Mr. A. R. Lytle

National Science Foundation
Engineering Mechanics Section
Division of Engineering
Washington, D.C. 20550

Picatinny Arsenal
Plastics Technical Evaluation Center
Attn: Technical Information Section
Dover, NJ 07810

Maritime Administration
Office of Maritime Technology
14th and Constitution Ave., NW.
Washington, D.C. 20230

PART 2 - Contractors and other Technical Collaborators

Universities

Dr. J. Tinsley Oden
University of Texas at Austin
345 Engineering Science Building
Austin, TX 78712

Professor Julius Miklowitz
California Institute of Technology
Division of Engineering
and Applied Sciences
Pasadena, CA 91109

Dr. Harold Liebowitz, Dean
School of Engineering and
Applied Science
George Washington University
Washington, D.C. 20052

Professor Eli Sternberg
California Institute of Technology
Division of Engineering and
Applied Sciences
Pasadena, CA 91109

Professor Paul M. Naghdi
University of California
Department of Mechanical Engineering
Berkeley, CA 94720

Professor A. J. Durelli
Oakland University
School of Engineering
Rochester, MO 48063

Professor F. L. DiMaggio
Columbia University
Department of Civil Engineering
New York, NY 10027

Professor Norman Jones
The University of Liverpool
Department of Mechanical Engineering
P.O. Box 147
Brownlow Hill
Liverpool L69 3BX
England

Professor E. J. Skudrzyk
Pennsylvania State University
Applied Research Laboratory
Department of Physics
State College, PA 16801

Universities (Con't.)

Professor J. Klosner
Polytechnic Institute of New York
Department of Mechanical and
Aerospace Engineering
333 Jay Street
Brooklyn, NY 11201

Prof. R. A. Schapery
Texas A&M University
Department of Civil Engineering
College Station, TX 77843

Professor Walter D. Pilkey
University of Virginia
Research Laboratories for the
Engineering Sciences and
Applied Sciences
Charlottesville, VA 22901

Professor K. D. Willmert
Clarkson College of Technology
Department of Mechanical Engineering
Potsdam, NY 13676

Dr. Walter E. Haisler
Texas A&M University
Aerospace Engineering Department
College Station, TX 77843

Dr. Hussein A. Kamel
University of Arizona
Department of Aerospace and
Mechanical Engineering
Tucson, AZ 85721

Dr. S. J. Fenves
Carnegie-Mellon University
Department of Civil Engineering
Schenley Park
Pittsburgh, PA 15213

Dr. Ronald L. Huston
Department of Engineering Analysis
University of Cincinnati
Cincinnati, OH 45221

Universities (Con't.)

Professor G. C. M. Sih
Lehigh University
Institute of Fracture and
Solid Mechanics
Bethlehem, PA 18015

Professor Albert S. Kobayashi
University of Washington
Department of Mechanical Engineering
Seattle, WA 98105

Professor Daniel Frederick
Virginia Polytechnic Institute and
State University
Department of Engineering Mechanics
Blacksburg, VA 24061

Professor A. C. Eringen
Princeton University
Department of Aerospace and
Mechanical Sciences
Princeton, NJ 08540

Professor E. H. Lee
Stanford University
Division of Engineering Mechanics
Stanford, CA 94305

Professor Albert I. King
Wayne State University
Biomechanics Research Center
Detroit, MI 48202

Dr. V. R. Hodgson
Wayne State University
School of Medicine
Detroit, MI 48202

Dean B. A. Boley
Northwestern University
Department of Civil Engineering
Evanston, IL 60201

Universities (Con't.)

Professor P. G. Hodge, Jr.
University of Minnesota
Department of Aerospace Engineering
and Mechanics
Minneapolis, MN 55455

Dr. D. C. Drucker
University of Illinois
Dean of Engineering
Urbana, IL 61801

Professor N. J. Newmark
University of Illinois
Department of Civil Engineering
Urbana, IL 61803

Professor E. Reissner
University of California, San Diego
Department of Applied Mechanics
La Jolla, CA 92037

Professor William A. Nash
University of Massachusetts
Department of Mechanics and
Aerospace Engineering
Amherst, MA 01002

Professor G. Herrmann
Stanford University
Department of Applied Mechanics
Stanford, CA 94305

Professor J. D. Achenbach
Northwest University
Department of Civil Engineering
Evanston, IL 60201

Professor S. B. Dong
University of California
Department of Mechanics
Los Angeles, CA 90024

Professor Burt Paul
University of Pennsylvania
Towne School of Civil and
Mechanical Engineering
Philadelphia, PA 19104

Universities (Con't.)

Professor H. W. Liu
Syracuse University
Department of Chemical Engineering
and Metallurgy
Syracuse, NY 13210

Professor S. Bodner
Technion R&D Foundation
Haifa, Israel

Professor Werner Goldsmith
University of California
Department of Mechanical Engineering
Berkeley, CA 94720

Professor R. S. Rivlin
Lehigh University
Center for Application
of Mathematics
Bethlehem, PA 18015

Professor F. A. Cozzarelli
State University of New York at
Buffalo
Division of Interdisciplinary Studies
Karr Parker Engineering Building
Chemistry Road
Buffalo, NY 14214

Professor Joseph L. Rose
Drexel University
Department of Mechanical Engineering
and Mechanics
Philadelphia, PA 19104

Professor B. K. Donaldson
University of Maryland
Aerospace Engineering Department
College Park, MD 20742

Professor Joseph A. Clark
Catholic University of America
Department of Mechanical Engineering
Washington, D.C. 20064

Universities (Con't.)

Dr. Samuel B. Batdorf
University of California
School of Engineering
and Applied Science
Los Angeles, CA 90024

Professor Isaac Fried
Boston University
Department of Mathematics
Boston, MA 02215

Professor E. Krempl
Rensselaer Polytechnic Institute
Division of Engineering
Engineering Mechanics
Troy, NY 12181

Dr. Jack R. Vinson
University of Delaware
Department of Mechanical and Aerospace
Engineering and the Center for
Composite Materials
Newark, DE 19711

Dr. J. Duffy
Brown University
Division of Engineering
Providence, RI 02912

Dr. J. L. Swedlow
Carnegie-Mellon University
Department of Mechanical Engineering
Pittsburgh, PA 15213

Dr. V. K. Varadan
Ohio State University Research Foundation
Department of Engineering Mechanics
Columbus, OH 43210

Dr. Z. Hashin
University of Pennsylvania
Department of Metallurgy and
Materials Science
College of Engineering and
Applied Science
Philadelphia, PA 19104

Universities (Con't.)

Dr. Jackson C. S. Yang
University of Maryland
Department of Mechanical Engineering
College Park, MD 20742

Professor T. Y. Chang
University of Akron
Department of Civil Engineering
Akron, OH 44325

Professor Charles W. Bert
University of Oklahoma
School of Aerospace, Mechanical,
and Nuclear Engineering
Norman, OK 73019

Professor Satya N. Atluri
Georgia Institute of Technology
School of Engineering and
Mechanics
Atlanta, GA 30332

Professor Graham F. Carey
University of Texas at Austin
Department of Aerospace ENgineering
and Engineering Mechanics
Austin, TX 78712

Dr. S. S. Wang
University of Illinois
Department of Theoretical and
Applied Mechanics
Urbana, IL 61801

Industry and Research Institutes

Dr. Norman Hobbs
Kaman AviDyne
Division of Kaman
Sciences Corporation
Burlington, MA 01803

Argonne National Laboratory
Library Services Department
9700 South Cass Avenue
Argonne, IL 60440

Industry and Research Institutes (Con't.)

Dr. M. C. Junger
Cambridge Acoustical Associates
54 Rindge Avenue Extension
Cambridge, MA 02140

Dr. V. Godino
General Dynamics Corporation
Electric Boat Division
Groton, CT 06340

Dr. J. E. Greenspon
J. G. Engineering Research Associates
3831 Menlo Drive
Baltimore, MD 21215

Newport News Shipbuilding and
Dry Dock Company
Library
Newport News, VA 23601

Dr. W. F. Bozich
McDonnell Douglas Corporation
5301 Bolsa Avenue
Huntington Beach, CA 92647

Dr. H. N. Abramson
Southwest Research Institute
8500 Culebra Road
San Antonio, TX 78284

Dr. R. C. DeHart
Southwest Research Institute
8500 Culebra Road
San Antonio, TX 78284

Dr. M. L. Baron
Weidlinger Associates
110 East 59th Street
New York, NY 10022

Dr. T. L. Geers
Lockheed Missiles and Space Company
3251 Hanover Street
Palo Alto, CA 94304

Mr. William Caywood
Applied Physics Laboratory
Johns Hopkins Road
Laurel, MD 20810

Industry and Research Institutes (Con't.)

Dr. Robert E. Dunham
Pacifica Technology
P.O. Box 148
Del Mar, CA 92014

Dr. M. F. Kanninen
Battelle Columbus Laboratories
505 King Avenue
Columbus, OH 43201

Dr. A. A. Hochrein
Daedalean Associates, Inc.
Springlake Research Road
15110 Frederick Road
Woodbine,, MD 21797

Dr. James W. Jones
Swanson Service Corporation
P.O. Box 5415
Huntington Beach, CA 92646

Dr. Robert E. Nickell
Applied Science and Technology
3344 North Torrey Pines Court
Suite 220
La Jolla, CA 92037

Dr. Kevin Thomas
Westinghouse Electric Corp.
Advanced Reactors Division
P.O. Box 158
Madison, PA 15663

Dr. Bernard Shaffer
Polytechnic Institute of New York
Dept. of Mechanical and Aeruspace
Engineering
333 Jay Street
Brooklyn,, NY 11021

Unclassified

SECURITY CLASSIFICATION OF THIS PAGE (When Data Entered)

REPORT DOCUMENTATION PAGE

READ INSTRUCTIONS BEFORE COMPLETING FORM

1. REPORT NUMBER: WA/DME/TR-83/48
2. GOVT ACCESSION NO.: AD-A130719
3. RECIPIENT'S CATALOG NUMBER:
4. TITLE (and Subtitle): Advanced Experimental Technique in Crack Tip Mechanics
5. TYPE OF REPORT & PERIOD COVERED: Technical Report
6. PERFORMING ORG. REPORT NUMBER: UWA/DME/TR-83/47
7. AUTHOR(s): A. S. Kobayashi
8. CONTRACT OR GRANT NUMBER(s): N00014-76-C-0060
9. PERFORMING ORGANIZATION NAME AND ADDRESS: Department of Mechanical Engineering FU-10, University of Washington, Seattle, WA 98195
10. PROGRAM ELEMENT, PROJECT, TASK AREA & WORK UNIT NUMBERS: NR 0640478
11. CONTROLLING OFFICE NAME AND ADDRESS: Office of Naval Research, Arlington, VA 22217
12. REPORT DATE: June 1983
13. NUMBER OF PAGES: 24
14. MONITORING AGENCY NAME & ADDRESS (if different from Controlling Office):
15. SECURITY CLASS. (of this report): Unclassified
15a. DECLASSIFICATION/DOWNGRADING SCHEDULE:
16. DISTRIBUTION STATEMENT (of this Report): Unlimited

This document has been approved for public release and sale; its distribution is unlimited.

17. DISTRIBUTION STATEMENT (of the abstract entered in Block 20, if different from Report):
18. SUPPLEMENTARY NOTES:
19. KEY WORDS (Continue on reverse side if necessary and identify by block number): Photoelasticity, caustics, moire method, isodyne photoelasticity, acousto-elasticity, fracture mechanics
20. ABSTRACT (Continue on reverse side if necessary and identify by block number):

Advanced experimental techniques in crack tip mechanics are discussed under three categories of 2- and 3-D linear elastic, 2-D elasto-plastic and 2-D dynamic fracture mechanics. Specific techniques which were discussed are acousto-elasticity, frozen stress-moire technique, isodyne photoelasticity, moire technique, laser speckle method, hybrid experimental-numerical analysis and caustic method.

DD FORM 1 JAN 73 1473 EDITION OF 1 NOV 65 IS OBSOLETE
S/N 0102-014-6601

Unclassified

SECURITY CLASSIFICATION OF THIS PAGE (When Data Entered)